Synthesis and Characterisation of a Phosphido-bridged Ruthenium Cluster: Crystal and Molecular Structure of $[Ru_5C(\mu\text{-}H)(\mu\text{-}PPh_2)(CO)_{13}]$†

Stephen L. Cook, John Evans,* Leslie R. Gray, and Michael Webster*
Department of Chemistry, The University, Southampton SO9 5NH

The complex $[Ru_5C(\mu\text{-}H)(\mu\text{-}PPh_2)(CO)_{13}]$ (**3**) has been prepared in a two-step synthesis from $[Ru_5C(CO)_{15}]$ and PPh_2H and crystallises in the monoclinic space group *C*2/*c*, with $a = 24.236(7)$, $b = 9.699(2)$, $c = 27.424(5)$ Å, $\beta = 99.54(2)°$, and $Z = 8$. The structure was refined to $R = 0.0535$ for 4 551 observed reflections. In the crystal, the complex contains a square pyramid of ruthenium atoms with the phosphido group bridging a basal edge [Ru-P 2.298(2), 2.314(2) Å]. The bridged edge [2.721(1) Å] is 0.15 Å shorter than any other basal Ru–Ru distance in the metal cage. An analogue of (**3**) was prepared from $PPh(H)CH_2CH_2Si(OEt)_3$ and $[Ru_5C(CO)_{15}]$. The limiting low-temperature ^{13}C n.m.r. spectrum of this complex, (**5**), showed the absence of any symmetry in solution and at least three CO-exchange processes at higher temperature. Complex (**5**) was tethered to silica and alumina *via* the silyl group. While (**5**) was reasonably stable on silica, decomposition on alumina occurred readily.

As part of our work to tether transition metal clusters to oxide supports,[1] we have investigated the reactions of $[Ru_5C(CO)_{15}]$ (**1**) with secondary phosphines. This system was chosen for three reasons. First, complex (**1**) will accept additional ligands which can be accommodated by a skeletal rearrangement;[2] this incipient unsaturation is a primary requirement for catalytic behaviour. Secondly, the interstitial carbide atom may stabilise the cluster core and, thirdly, this stability would be expected to be enhanced by a bridging phosphido group.[3]

Experimental

Infrared and u.v.-visible spectra were recorded on Perkin-Elmer 580B and 554 spectrometers respectively. Hydrogen-1 and carbon-13 (25.2 MHz) n.m.r. spectra were obtained on a Varian XL-100, while 90-MHz ^{13}C n.m.r. spectra were recorded on a Bruker WH-360 spectrometer at Edinburgh University. Phosphorus-31 n.m.r. spectra were recorded on a Bruker AM-360 spectrometer.

Diphenylphosphine,[4] $PPhH_2$,[5] and $[Ru_5C(CO)_{15}]$[6] were prepared by published procedures. The samples of silica (Aerosil 380) and alumina (Aluminoxid C) were supplied by Degussa and dried at 150 °C *in vacuo* before use.

Unless otherwise stated, reactions were performed under nitrogen.

Reaction of $[Ru_5C(CO)_{15}]$ (**1**) *with* PPh_2H.—A solution of complex (**1**) (0.100 g, 0.1 mmol) in n-pentane (125 cm^3) was cooled in a methanol slush bath. PPh_2H (22 μl) was added and the mixture allowed to warm to room temperature. The solution was mixed with Merck silica gel 60. Elution from a column (1 × 40 cm) with CH_2Cl_2–light petroleum (b.p. 40—60 °C; 1:9 v/v) afforded the product, $[Ru_5C(CO)_{14}(PPh_2H)]$ (**2**) (0.083 g, 71%). I.r.: ν(CO)(cyclohexane) at 2 089m, 2 057vs, 2 048s, 2 026s, 2 019s, and 1 991m cm^{-1}. ^1H N.m.r. ($CDCl_3$): δ 7.36 (m, 10 H, Ph) and 6.42 [d,1 H,P-H,*J*(PH) 371 Hz].

Preparation of $[Ru_5C(\mu\text{-}H)(\mu\text{-}PPh_2)(CO)_{13}]$ (**3**).—A solution of complex (**2**) (0.083 g, 76 μmol) in hexane (50 cm^3) was refluxed for 2 h, during which time the solution changed from purple to orange. The product was isolated by flash chromatography from silica using light petroleum (b.p. 40—60 °C) as eluant. The product was obtained as orange red crystals; yield 64 mg (80%) (Found: C, 29.1; H, 1.2. Calc. for $C_{26}H_{11}O_{13}PRu_5$: C, 29.2; H, 1.0%. I.r.: ν(CO) (cyclohexane) at 2 088m, 2 057s, 2 042vs, 2 034s, 2 019m, 2 003w, 1 994m, 1 974w, and 1 967w (sh) cm^{-1}. N.m.r. ($CDCl_3$): ^1H, δ 7.44 (m,10 H,Ph) and −22.16 [d,1 H,Ru-H,*J*(PH) 2 Hz]. $^{31}P\text{-}\{^1H\}$, δ 267.26.

Preparation of $PPh(H)CH_2CH_2Si(OEt)_3$.—A solution of $CH_2{=}CHSi(OEt)_3$ (29 cm^3, 94 mmol) and $PPhH_2$ (11.5 cm^3, 110 mmol) in heptane (45 cm^3) was irradiated with a medium-pressure Hg lamp through Pyrex for 112 h. The product was isolated as a colourless oil (12.7 g, 45%) by distillation (b.p. 140—144 °C, 0.65 mmHg); M^+, *m/e* 300. ^1H N.m.r. ($CDCl_3$): δ 7.3 (m,5 H,Ph), 3.75 (q,6 H,*O*-CH_2), 1.8 (m,2 H,*P*-CH_2), 1.1 (t,9 H,Me), and 0.7 (m,2 H,Si-CH_2).

Reaction of (**1**) *with* $PPh(H)CH_2CH_2Si(OEt)_3$.—This was performed as for the reaction with PPh_2H. The product, $[Ru_5C(CO)_{14}\{PPh(H)CH_2CH_2Si(OEt)_3\}]$ (**4**), was isolated by flash chromatography using CH_2Cl_2–light petroleum (b.p. 40—60 °C; 1:1 v/v) (yield 34%). I.r.: ν(CO) (cyclohexane) 2 088m, 2 055vs, 2 043m, 2 034m, 2 023s, 2 017s, and 1 992m cm^{-1}.

Conversion of (**4**) *to* $[Ru_5C(\mu\text{-}H)\{\mu\text{-}P(Ph)CH_2CH_2Si(OEt)_3\}(CO)_{13}]$ (**5**).—This was carried out as for the preparation of (**3**), with the isolation of (**5**) by the method described for (**4**). Complex (**5**) was obtained as an orange oil (87%). I.r.: ν(CO) at 2 088m, 2 055s, 2 041s, 2 034s, 2 018m, 2 002w, 1 993m, and 1 973w cm^{-1}. N.m.r.: ^1H ($CDCl_3$), δ 7.5 (m,5 H,Ph), 3.76 (q,6 H,*O*-CH_2), 2.90 (m,2 H,*P*-CH_2), 1.18 (t,9 H,Me), 0.90 (m,2 H,Si-CH_2), and −22.23 [d,1 H,Ru-H,*J*(PH) 2 Hz]. $^{13}C\text{-}\{^1H\}$ (25.2 MHz), δ 210.93, 200.28, 199.66, 197.32, 195.60, 193.86, 193.21, 191.88, 191.43, 188.94, 186.12 (all CO, relative intensities 1:1:1:1:1:2:2:1:1:1:1), 132.41—128.50 (Ph carbons), 56.68 (*O*-CH_2), 37.43 [d,*P*-CH_2,*J*(PC) 15 Hz], 18.21 (Me), and 10.12 [d,Si-CH_2,*J*(PC) 7 Hz].

Interaction of (**5**) *with Silica and Alumina*.—Aliquots (12.5 cm^3) of a solution of complex (**5**) in CH_2Cl_2 (1.2 g dm^{-3}) were added to suspensions of the oxides (0.3 g) in CH_2Cl_2 (20 cm^3).

---

† μ_5-Carbido-1,1,1,2,2,2,3,3,3,4,4,5,5-tridecacarbonyl-4,5-μ-diphenylphosphido-1,2-μ-hydrido-*cyclo*-pentaruthenium(8 *Ru*–*Ru*).

Supplementary data available (No. SUP 56574, 5 pp.): thermal parameters, H-atom co-ordinates, packing diagram. See Instructions for Authors, *J. Chem. Soc., Dalton Trans.*, 1986, Issue 1, pp. xvii–xx. Structure factors are available from the editorial office.

Non-S.I. unit employed: mmHg ≈ 133 N m^{-2}.

Table 1. Final atomic co-ordinates (× 10^4)

Atom	*x*	*y*	*z*
Ru(1)	3 036.2(3)	1 500.4(8)	883.6(3)
Ru(2)	3 563.3(3)	−966.8(7)	1 324.1(3)
Ru(3)	4 249.8(3)	1 184.3(8)	1 206.2(3)
Ru(4)	3 573.6(3)	3 040.7(8)	1 680.8(3)
Ru(5)	2 897.4(3)	718.0(8)	1 863.7(3)
P	4 258(1)	−972(2)	847(1)
C(0)	3 598(4)	1 002(9)	1 562(3)
C(1)	3 435(4)	2 261(11)	409(4)
O(1)	3 593(4)	2 825(10)	93(3)
C(2)	2 683(5)	138(12)	430(4)
O(2)	2 432(4)	−613(10)	157(4)
C(3)	2 525(5)	3 013(12)	790(4)
O(3)	2 202(4)	3 891(10)	731(4)
C(4)	3 897(4)	−2 141(11)	1 820(4)
O(4)	4 087(4)	−2 868(10)	2 132(4)
C(5)	3 099(4)	−2 416(11)	1 049(4)
O(5)	2 805(4)	−3 309(9)	875(3)
C(6)	4 656(4)	2 310(11)	828(4)
O(6)	4 895(4)	3 032(9)	600(3)
C(7)	4 878(5)	980(12)	1 671(4)
O(7)	5 253(5)	842(11)	1 990(4)
C(8)	4 022(6)	3 403(14)	2 287(5)
O(8)	4 302(5)	3 610(14)	2 677(5)
C(9)	3 943(5)	4 318(12)	1 327(4)
O(9)	4 123(5)	5 140(12)	1 089(4)
C(10)	3 017(5)	4 294(11)	1 811(4)
O(10)	2 679(4)	5 063(10)	1 897(4)
C(11)	2 321(4)	1 791(11)	2 070(4)
O(11)	1 956(4)	2 429(10)	2 182(3)
C(12)	2 490(5)	−955(11)	1 822(4)
O(12)	2 208(4)	−1 900(9)	1 811(3)
C(13)	3 289(4)	447(11)	2 515(4)
O(13)	3 539(4)	320(9)	2 904(3)
C(21)	4 854(2)	−2 133(7)	985(2)
C(22)	5 117(2)	−2 292(7)	1 474(2)
C(23)	5 573(2)	−3 181(7)	1 586(2)
C(24)	5 766(2)	−3 911(7)	1 209(2)
C(25)	5 502(2)	−3 751(7)	720(2)
C(26)	5 046(2)	−2 862(7)	608(2)
C(31)	4 050(3)	−1 133(7)	179(2)
C(32)	3 744(3)	−2 283(7)	−15(2)
C(33)	3 602(3)	−2 446(7)	−525(2)
C(34)	3 767(3)	−1 459(7)	−843(2)
C(35)	4 073(3)	−309(7)	−649(2)
C(36)	4 214(3)	−146(7)	−138(2)

These suspensions were stirred under CO (1 atm) until the solution was decolourised. The reaction times were 20 h and 3 d for alumina and silica respectively. The oxides were isolated by filtration, washed with CH_2Cl_2 and acetone, and dried *in vacuo*. The loadings on the supports were 20 mg and 40 mg of (**5**) per gram of oxide for alumina and silica respectively.

Crystal Structure Determination.—Orange-red block shaped crystals of complex (**3**) were obtained from pentane solution by a slow evaporation under N_2. Preliminary photographic measurements gave the cell dimensions and crystal system.

Crystal data. $C_{26}H_{11}O_{13}PRu_5$, $M = 1\,067.7$, monoclinic, $a = 24.236(7)$, $b = 9.699(2)$, $c = 27.424(5)$ Å, $\beta = 99.54(2)°$, $U = 6\,357.7$ Å^3, $D_m = 2.23(2)$ g cm^{-3} (flotation), $Z = 8$, $D_c = 2.230$, $F(000) = 4\,048$, space group $C2/c$, λ(Mo-K_α) = 0.7107 Å, μ(Mo-K_α) = 23.58 cm^{-1}.

Accurate cell dimensions were obtained from 25 accurately centred reflections on an Enraf-Nonius CAD-4 diffractometer equipped with graphite-monochromated Mo-K_α radiation. From a room-temperature crystal (0.5 × 0.5 × 0.35 mm) were recorded 6 308 reflections [$1.5 \leqslant \theta \leqslant 25°$; h(0—28), k(0—11), l(−32 to +32)] including three check reflections. No decomposition was observed during the experiment. Systematic absences [hkl, $h + k \neq 2n$, $h0l$, $l \neq 2n$ ($h \neq 2n$)] led to space group Cc or $C2/c$ of which the latter was indicated by the normalised structure factors and confirmed by the structure solution. After data reduction there remained 5 605 unique reflections, and omitting those where $F < 6\sigma(F)$ left 4 555 reflections used for the structure solution and refinement. No absorption correction was applied to the data.

Structure determination. The five ruthenium atoms were located from the direct methods facility in SHELX[7] (EEES, parachor 4.38). The remaining atoms were located by repeated structure factor and electron-density syntheses. The phenyl groups were constrained as rigid groups (C–C 1.395 Å). Some evidence for phenyl-H atoms was found in the difference electron-density synthesis and these were introduced in geometrically calculated positions (C–H 0.95 Å) with a common refined thermal parameter. Four reflections appeared to suffer from extinction and these were removed. Full matrix least-squares refinement {4 551 reflections, anisotropic (Ru, P) and isotropic (O,C,H) atoms, $w = 1/[\sigma^2(F) + 0.0002F^2]$, 188 parameters, reflections/parameters = 24.2, maximum shift/error 0.2} converged to $R = 0.0535$ ($R' = 0.0769$). A final difference electron-density synthesis showed all features in the range 1.38 to −1.96 e Å^{-3} but no persuasive hydride position was identified.

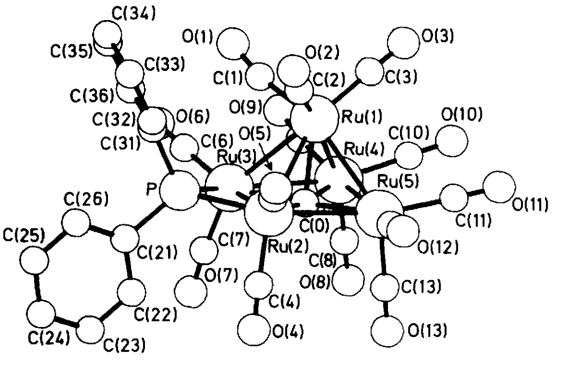

Figure 1. Discrete molecule of $[Ru_5C(\mu\text{-}H)(\mu\text{-}PPh_2)(CO)_{13}]$ showing the atom numbering scheme and with H atoms excluded for clarity

Scattering factors for neutral atoms and anomalous dispersion terms were taken from the literature[8] (Ru) or SHELX.[7] Final atomic co-ordinates, selected bond lengths and bond angles are presented in Tables 1—3. Diagrams were produced using the program PLUTO[9] and all calculations were performed using an ICL 2970 computer.

Results and Discussion

As has been reported for tertiary phosphines,[2,10] PPh_2H forms a substitution product when allowed to react with $[Ru_5C(CO)_{15}]$ (**1**) under mild conditions. Infrared evidence suggests that the phosphine in the product (**2**) adopts the same co-ordination site as in $[Ru_5C(CO)_{14}(PPh_3)]$ (**6**).[2,6] Mild thermolysis caused the loss of a second carbonyl group accompanied by the metallation of the hydrogen attached to phosphorus to form complex (**3**), shown by *X*-ray diffraction

Table 2. Selected bond lengths (Å) for $[Ru_5C(\mu\text{-}H)(\mu\text{-}PPh_2)(CO)_{13}]$ (**3**)

Ru(1)–Ru(2)	2.882(1)	Ru(2)–Ru(3)	2.721(1)
Ru(1)–Ru(3)	2.944(1)	Ru(2)–Ru(5)	2.873(1)
Ru(1)–Ru(4)	2.786(1)	Ru(3)–Ru(4)	2.886(1)
Ru(1)–Ru(5)	2.866(1)	Ru(4)–Ru(5)	2.878(1)
Ru(1)–C(0)	2.17(1)	Ru(4)–C(0)	2.01(1)
Ru(2)–C(0)	2.02(1)	Ru(5)–C(0)	2.03(1)
Ru(3)–C(0)	2.00(1)		
Ru(2)–P	2.298(2)	P–C(21)	1.820(6)
Ru(3)–P	2.314(2)	P–C(31)	1.824(5)
C–O (max.)	1.19(2)	Ru–C (max.)	1.92(1)
C–O (min.)	1.14(1)	Ru–C (min.)	1.83(1)
C–O (mean)	1.16(1)	Ru–C (mean)	1.88(1)
C–C (fixed)	1.395		

and n.m.r. to be $[Ru_5C(\mu\text{-}H)(\mu\text{-}PPh_2)(CO)_{13}]$. Interaction of (**1**) with $PPhH_2$ caused the formation of $[Ru_5C(\mu\text{-}H)(\mu\text{-}PPhH)(CO)_{13}]$ even at room temperature. Two ^{31}P chemical shifts were observed for this complex (δ 196.1 and 196.7), suggesting that there were two isomers formed, differing in the relative orientations of the phenyl and hydrogen groups on the bridging phenylphosphido ligand. Attempts were made to induce a second abstraction of a P–H bond to form a phosphinidene cluster. However, neither thermal nor chemical (Me_3NO or Na/Ph_2CO) methods were successful.

Structure of Complex (**3**).—The cluster is based on a square pyramid of ruthenium atoms with an interstitial carbon (Figure 1), as observed for the parent $[Ru_5C(CO)_{15}]$ which has the same skeletal electron count. The PPh_2 ligand forms a slightly asymmetric bridge on a basal edge. As in the case of $[Ru_5C(\mu\text{-}H)(\mu\text{-}SEt)(CO)_{12}(PPh_3)]$ (**7**),[10] the bridge is in a radial orientation, rather than the axial sites adopted by phosphine ligands in (**6**), $[Ru_5C(CO)_{13}(PPh_3)_2]$ (**8**),[6] and $[Ru_5C(CO)_{13}\{PPh_2(CH_2)_4PPh_2\}]$ (**9**).[11] The hydride was not located. The ^{13}C n.m.r. spectrum of the tethering derivative (**5**) (see below) indicates only C_1 molecular symmetry in solution, so the hydride is unlikely to be associated with either the Ru(2)–Ru(3) or Ru(4)–Ru(5) edges. Two criteria for indirect hydride location are the length of the M–M vector and large M–M–C bond angles opening up space for the hydride in the ligand polyhedron. In the related complex (**7**), the longest Ru–Ru bond (3.024 Å)[10] spans an edge between the apex of the square pyramid and a basal metal atom associated with the thiolate bridge. The ligands around this edge, however, did not provide a cavity for the hydride and an alternative basal metal, remote from the thiolate bridge was favoured to be involved in the hydride bridge; the long Ru–Ru bond was *trans* to the Ru–PPh_3 bond in that complex.[10] The situation is similar for complex (**3**). Ru(1)–Ru(3) is the longest metal–metal vector (2.944 Å), but this also does not provide an obvious hydride site. The effect of the PPh_2 is to rotate the ML_3 units on Ru(2) and Ru(3) so that the remaining radial CO on these metal atoms is nearer to the direction of the apical-basal Ru–Ru bond. In complex (**3**), space is provided along the Ru(1)–Ru(5) edge, and the small value of *J*(P–H) (2 Hz) is consistent with this disposition remote from the phosphido bridge. The recent report[12] of the molecular structure of $[Ru_5C(\mu\text{-}H)_3(\mu\text{-}PPh_2)(CO)_{11}(PMePh_2)]$ (**10**) also supports this proposal. All three hydride ligands were located directly on three of the Ru–Ru edges to the apical metal atom; the one such edge remaining vacant is associated with a ruthenium involved in the PPh_2 bridge.

Table 3. Selected bond angles (°) for $[Ru_5C(\mu\text{-}H)(\mu\text{-}PPh_2)(CO)_{13}]$ (**3**)

Ru(1)–Ru(2)–P	94.5(1)	Ru(2)–P–C(21)	120.9(2)
Ru(1)–Ru(3)–P	92.6(1)	Ru(2)–P–C(31)	117.7(2)
Ru(2)–Ru(3)–P	53.6(1)	Ru(3)–P–C(21)	122.2(2)
Ru(3)–Ru(2)–P	54.1(1)	Ru(3)–P–C(31)	119.0(2)
Ru(5)–Ru(2)–P	145.3(1)	C(21)–P–C(31)	103.5(3)
Ru(4)–Ru(3)–P	143.3(1)	Ru(2)–P–Ru(3)	72.3(1)
Ru(1)–Ru(2)–Ru(3)	63.3(1)	Ru(3)–Ru(1)–Ru(4)	60.4(1)
Ru(1)–Ru(3)–Ru(2)	61.0(1)	Ru(4)–Ru(1)–Ru(5)	61.2(1)
Ru(1)–Ru(3)–Ru(4)	57.1(1)	Ru(2)–Ru(1)–Ru(5)	60.0(1)
Ru(1)–Ru(4)–Ru(3)	62.5(1)	Ru(2)–Ru(3)–Ru(4)	91.2(1)
Ru(1)–Ru(2)–Ru(5)	59.7(1)	Ru(3)–Ru(4)–Ru(5)	88.4(1)
Ru(1)–Ru(5)–Ru(2)	60.3(1)	Ru(4)–Ru(5)–Ru(2)	88.3(1)
Ru(1)–Ru(4)–Ru(5)	60.8(1)	Ru(5)–Ru(2)–Ru(3)	91.8(1)
Ru(1)–Ru(5)–Ru(4)	58.0(1)	Ru(2)–Ru(1)–Ru(4)	90.0(1)
Ru(2)–Ru(1)–Ru(3)	55.7(1)	Ru(3)–Ru(1)–Ru(5)	87.6(1)
Ru(2)–C(0)–Ru(4)	170.3(5)	Ru(1)–C(0)–Ru(5)	86.1(3)
Ru(3)–C(0)–Ru(5)	174.4(5)	Ru(2)–C(0)–Ru(3)	85.4(3)
Ru(1)–C(0)–Ru(2)	87.0(3)	Ru(3)–C(0)–Ru(4)	92.2(4)
Ru(1)–C(0)–Ru(3)	89.8(3)	Ru(4)–C(0)–Ru(5)	91.1(4)
Ru(1)–C(0)–Ru(4)	83.6(3)	Ru(5)–C(0)–Ru(2)	90.6(3)
Co-ordination at apical $Ru(CO)_3$ group			
C(1)–Ru(1)–C(2)	92.7(5)	C(1)–Ru(1)–C(3)	90.1(5)
C(2)–Ru(1)–C(3)	103.4(5)		
Co-ordination at basal $Ru(CO)_3$ groups			
C(8)–Ru(4)–C(9)	94.5(5)	C(11)–Ru(5)–C(12)	94.9(5)
C(8)–Ru(4)–C(10)	92.2(5)	C(11)–Ru(5)–C(13)	94.2(4)
C(9)–Ru(4)–C(10)	95.1(5)	C(12)–Ru(5)–C(13)	96.5(4)
Co-ordination at $Ru(CO)_2P$ groups			
C(4)–Ru(2)–C(5)	89.7(5)	C(6)–Ru(3)–C(7)	89.7(5)
C(4)–Ru(2)–P	98.3(3)	C(6)–Ru(3)–P	104.3(3)
C(5)–Ru(2)–P	102.5(3)	C(7)–Ru(3)–P	97.7(4)
Ru(1)–Ru(*n*)–C(axial)			
Ru(1)–Ru(2)–C(4)	157.9(3)	Ru(1)–Ru(4)–C(8)	158.3(4)
Ru(1)–Ru(3)–C(7)	153.7(4)	Ru(1)–Ru(5)–C(13)	143.3(3)
Ru(basal)–Ru(basal)–C(radial)			
Ru(3)–Ru(2)–C(5)	149.7(3)	Ru(2)–Ru(3)–C(6)	153.2(3)
Ru(5)–Ru(2)–C(5)	106.4(3)	Ru(4)–Ru(3)–C(6)	105.9(3)
Ru(3)–Ru(4)–C(9)	79.9(4)	Ru(2)–Ru(5)–C(12)	79.2(3)
Ru(5)–Ru(4)–C(9)	159.2(4)	Ru(4)–Ru(5)–C(12)	165.1(3)
Ru(5)–Ru(4)–C(10)	91.5(3)	Ru(4)–Ru(5)–C(11)	95.2(3)
Ru(3)–Ru(4)–C(10)	164.0(3)	Ru(2)–Ru(5)–C(11)	165.3(3)
Ru–C–O (max.)	179(1)		
Ru–C–O (min.)	169(1)		
Ru–C–O (mean)	176(3)		

Comparisons with the structural details of other square pyramidal pentaruthenium clusters are presented in Table 4. In complex (**3**) the carbide atom is 0.12 Å out of the basal Ru_4 plane, very similar to the observations on (**1**) and (**7**). In contrast, the presence of the axial phosphine substituents in (**6**), (**8**), and (**9**) results in the carbide moving a further 0.1 Å out of this plane.

The most evident parameter in complex (**3**) is the length of the phosphido-bridged metal–metal bond. At 2.721 Å this is 0.15 Å shorter than the remaining three basal metal–metal bonds and 0.14 Å shorter than those in $[Ru_5C(CO)_{15}]$. This effect is more marked in the thiolate-bridged bond in (**7**). The Ru–Ru and Ru–P distances in the Ru–PPh_2–Ru units of a series of clusters is presented in Table 5. There are examples of PPh_2-bridged Ru–Ru vectors varying by *ca.* 0.8 Å. In addition to supporting

Table 4. Structural features of Ru_5C cages

		Mean distances (Å)				
		Ru(apical)–Ru(basal)		Ru(basal)–Ru(basal)		
Complex	C–Ru_4 plane	unbridged	bridged	unbridged	bridged	Ref.
(**1**) $[Ru_5C(CO)_{15}]$	0.11	2.83		2.86		6
(**3**) $[Ru_5C(\mu\text{-}H)(\mu\text{-}PPh_2)(CO)_{13}]$	0.12	2.84	2.944	2.88	2.721	*
(**7**) $[Ru_5C(\mu\text{-}H)(\mu\text{-}SEt)(CO)_{12}(PPh_3)]$	0.12	2.85	3.024	2.86	2.698	10
(**10**) $[Ru_5C(\mu\text{-}H)_3(\mu\text{-}PPh_2)(CO)_{11}(PMePh_2)]$		2.88	2.87	2.90	2.771	12
(**6**) $[Ru_5C(CO)_{14}(PPh_3)]$	0.19	2.81		2.85		6
(**8**) $[Ru_5C(CO)_{13}(PPh_3)_2]$	0.23	2.81		2.86		6
(**9**) $[Ru_5C(CO)_{13}\{PPh_2(CH_2)_4PPh_2\}]$	0.21	2.82		2.87		11

* This work.

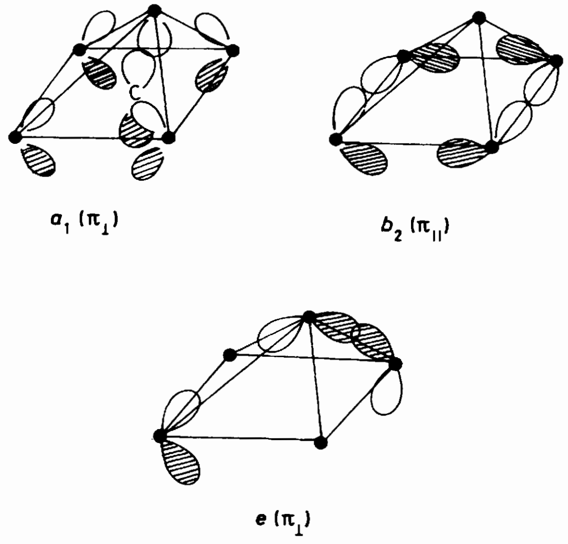

Figure 2. Some skeletal molecular orbitals of a $(ML_3)_5$ cage

metal centres with a normal Ru–Ru bonding distance (*ca.* 2.81—2.86 Å), gradations of more weakly and more strongly interacting atoms are also evident. There is no monotonic relationship between Ru–Ru and Ru–P distances. Complex (**3**) is one of a group of molecules exhibiting the unusually short Ru–Ru distance of *ca.* 2.70—2.73 Å, but which are electron precise based on the 'effective atomic number rule' (considered for the cluster overall). In three of these complexes the Ru_2P plane is approximately coplanar with the basal plane of an Ru_5 square pyramid [deviation 9.4° in (**3**)]; the phosphorus atom in complex (**3**) is 0.30 Å below the basal plane.

It is clear that there is an electronic preference for the bridging groups to occupy radial sites on the base of the square pyramid; the more bulky tertiary phosphine ligands adopt axial sites. This preference is accompanied by an apparent strengthening of the bridged Ru–Ru bond. Extended-Hückel molecular orbital calculations on $[Fe_5C(CO)_{15}]$ have been modelled by $(HFe)_5C$[13] and indicate that the frontier orbitals were largely metal in character (b_2 and e filled; b_1 empty); bonding orbitals of carbidic character were considerably lower in energy. This may in part account for the different preferences for bridging ligand sites on isolobal, square pyramidal $(BH)_5$ units. The favoured sites in the latter are below the basal plane (as in B_5H_9) and have been shown to result from strong interactions with the $\pi_\perp$ skeletal orbitals.[14] The bonding $\pi_\perp$ orbital (a_1) is likely to be primarily involved with the carbide $2p_z$ orbital, having other orbitals for interaction with the bridging groups (Figure 2). Of these, the b_2 orbital will be oriented around the basal plane, and therefore may form a secondary interaction between the PPh_2-bridged ruthenium atoms *via* the phosphorus atom. This interaction is larger in the thiolate cluster (**7**), suggesting the interaction is in the metal-to-ligand donation sense. A representative e skeletal orbital is depicted in Figure 2. This would principally involve interaction of the basal $\pi_\perp$ non-bonding orbitals with the apex. (The alternative largely basal-plane representation would be involved with the carbide $2p_x$ and $2p_y$ orbitals.) This orbital has good directional properties for interaction with a hydrogen bridging basal–apical ruthenium edges.

Table 5. Bond lengths in PPh_2-bridged Ru–Ru edges

	Mean bond lengths (Å)		
Complex	Ru–Ru	Ru–P	Ref.
$[Ru_5(C_2Ph)(PPh_2)(CO)_{13}]$	2.697	2.286	*a*
$[Ru_3(C_2Pr^i)(PPh_2)(CO)_8]$	2.709	2.337	*b*
$[Ru_5C(H)(PPh_2)(CO)_{13}]$ (**3**)	2.721	2.306	*c*
$[Ru_5(C_2PPh_2)(PPh_2)(CO)_{13}]$	2.731	2.316	*d*
$[Ru_2(C_2Bu^t)(PPh_2)(CO)_6]$	2.752	2.341	*e*
$[Ru_5C(H)_3(PPh_2)(CO)_{11}(PMePh_2)]$ (**10**)	2.771	2.307	12
$[Ru_3(C_6H_4)(PPh_2)_2(CO)_7]$	2.776	2.301	*f*
$[Ru_5H(C_2HPPh_2)(PPh_2)(CO)_{13}]$	2.781	2.305	12
$[Ru_2(C_2Pr^i)(PPh_2)(PPh_2C_2Pr^i)(CO)_5]$	2.795	2.339	*e*
$[Ru_3H(PPh_2)_3(CO)_7]$	2.807	2.337	*g*
$[Ru_5(C_2Ph)(PPh_2)(CO)_{14}]$	2.845	2.310	*a*
$[Ru_3(C_2Bu^t)_2(PPh_2)_2(PPh_2C_2Bu^t)(CO)_6]$	2.863	2.328	*e*
$[Ru_3H(PPh_2)(CO)_9]$	2.905	2.334	*h*
$[Ru_3(C_6H_4)(PPh_2)(CO)_7]$	2.956	2.340	*f*
$[Ru_5P(PPh_2)(CO)_{16}]$	2.968		*i*
$[Ru_3H(PPh_2)_3(CO)_7]$	2.985	2.362	*g*
$[Ru_4(C_2Bu^t)_2(PPh_2)_2(PPh_2C_2Bu^t)(CO)_8]$	3.060	2.353	*e*
$[Ru_4(C_2Bu^t)(PPh_2)(CO)_{13}]$	3.197	2.312	*e*
$[Ru_3(C_2Pr^i)(PPh_2)(CO)_9]$	3.466	2.393	*b, e*

[a] S. A. McLaughlin, N. J. Taylor, and A. J. Carty, *Organometallics*, 1983, **2**, 1194. [b] A. J. Carty, S. A. McLaughlin, and N. J. Taylor, *J. Organomet. Chem.*, 1981, **204**, C27. [c] This work. [d] M. I. Bruce, M. L. Williams, J. M. Patrick, and A. H. White, *J. Chem. Soc., Dalton Trans.*, 1985, 1229. [e] A. J. Carty, *Pure Appl. Chem.*, 1982, **54**, 115. [f] M. I. Bruce, J. M. Guss, R. Mason, B. W. Skelton, and A. H. White, *J. Organomet. Chem.*, 1983, **251**, 261. [g] R. P. Rosen, G. L. Geoffroy, C. Bueno, M. R. Churchill, and R. B. Otega, *J. Organomet. Chem.*, 1983, **254**, 89. [h] S. A. McLaughlin, A. J. Carty, and N. J. Taylor, *Can. J. Chem.*, 1982, **60**, 87. [i] S. A. McLaughlin, A. J. Carty, and N. J. Taylor, *Inorg. Chem.*, 1983, **22**, 1409.

Table 6. Infrared and u.v.–visible data on $[Ru_5C(\mu\text{-}H)\{\mu\text{-}P(Ph)CH_2CH_2Si(OEt)_3\}(CO)_{13}]$ (**5**) in solution and on oxide supports

Medium	$\nu(CO)/cm^{-1}$	U.v.–visible (λ/nm)[b]
Solution[a]	2 088m, 2 055s, 2 041s, 2 034s, 2 018m, 2 002w, 1 993m, 1 973w	465, 320, 228
Silica	2 088m, 2 055s, 2 039vs, 2 035s, 2 017m, 2 000w, 1 992w, 1 971vw	470, 457, 330, 256
Alumina	2 088w, 2 056vs, 2 042s, 2 036s, 2 015vs, 2 004vs, 1 990vs, 1 970m (sh)	500, 468, 425, 315, 228

[a] Solution in cyclohexane. [b] Solution in CH_2Cl_2.

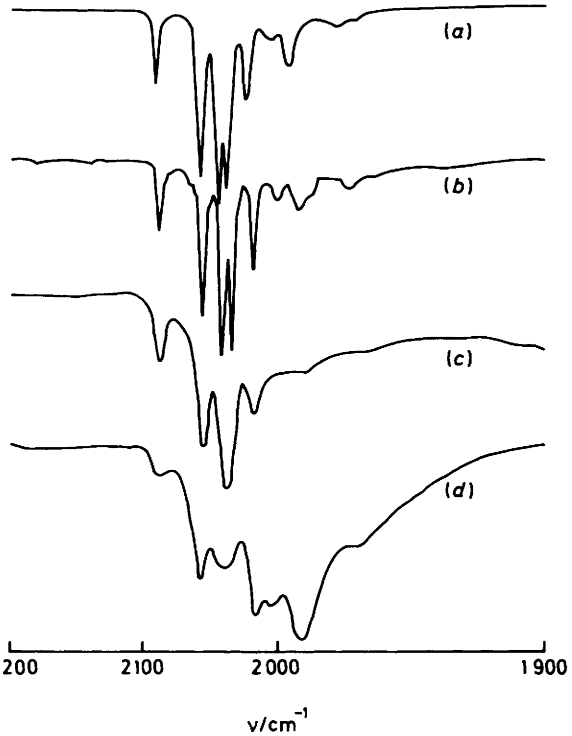

Figure 3. Infrared spectra in the ν(CO) region of (*a*) (**3**) in cyclohexane, (*b*) (**5**) in cyclohexane, (*c*) (**5**) on silica (in Nujol), and (*d*) (**5**) on alumina (in Nujol)

A Tethered Version of Complex (**3**).—Reaction of $[Ru_5C(CO)_{15}]$ with $PPh(H)CH_2CH_2Si(OEt)_3$ followed by mild thermolysis afforded an oily solid which was characterised spectroscopically as containing $[Ru_5C(\mu\text{-}H)\{\mu\text{-}P(Ph)CH_2CH_2\text{-}Si(OEt)_3\}(CO)_{13}]$ (**5**); i.r., ^1H and ^{13}C n.m.r. spectra were all consistent with this complex being a close derivative of (**3**). A variable-temperature ^{13}C n.m.r. study was carried out on a ^{13}CO-enriched (*ca.* 10%) sample of (**5**). The limiting low-temperature spectrum of the ^{13}CO region indicated that the complex was unsymmetrical; 11 lines were resolved between δ 211 and 186 at 25.2 MHz, with one of the two accidental degeneracies removed at 90.56 MHz. Spectra were obtained from −75 to 44 °C. At −54 °C the three resonances at δ 199.52, 197.41, and 188.93 broaden. This suggests that the $Ru(CO)_3$ group in the apical site is undergoing a localised rotation; this was found to be the lowest energy exchange process in (**1**) and (**9**).[15] At −26 °C, the remaining resonances all broaden in an apparently single process. This is probably the hydride exchange generating a pseudo-mirror plane. At 34 °C the first process is rapid, but a third type of exchange is evident at 44 °C. Decomposition at 66 °C precluded spectra at higher temperatures.

Complex (**5**) was interacted with silica and alumina under a CO atmosphere, the uptake of the complex being more rapid on alumina. The nature of the species on the oxide surfaces was studied by i.r. and electronic spectroscopy (Table 6); a comparison of the partial i.r. spectra in the ν(CO) region is given in Figure 3. It is evident that the predominant species on silica is a tethered version of (**5**). This material could be stored for *ca.* 6 months at −20 °C with little decomposition. However, the alumina-supported variant exhibits extra i.r. intensity at 2 056, 2 015, 2 004, and 1 990 cm^{-1}. There are also additional bands in the electronic reflectance spectrum at 500 and 425 nm. All traces of (**5**) were lost after 6 months at −20 °C. The presence of the phosphido and carbido groups evidently does not confer substantial stability on the cluster unit in this case. Considerably greater stability on alumina was displayed by $[Ru_3(\mu\text{-}H)_2\{\mu_3\text{-}PCH_2CH_2Si(OEt)_3\}(CO)_9]$,[16] where the cluster is supported by a face-bridging ligand.

Acknowledgements

We wish to thank Dr. I. H. Sadler and Mrs. J. M. Street for n.m.r. spectra, the S.E.R.C. and the University of Southampton for support (to S.L.C. and L.R.G. respectively), Johnson Matthey for the loan of ruthenium trichloride, Degussa for the oxide samples, and Dr. M. B. Hursthouse for the *X*-ray data collection on the Q.M.C./S.E.R.C. diffractometer.

References

1 S. C. Brown, J. Evans, and M. Webster, *J. Chem. Soc., Dalton Trans.*, 1981, 2263; J. Evans and B. P. Gracey, *J. Chem. Soc., Chem. Commun.*, 1983, 247.
2 D. H. Farrar, P. F. Jackson, B. F. G. Johnson, J. Lewis, J. N. Nicholls, and M. McPartlin, *J. Chem. Soc., Chem. Commun.*, 1981, 415.
3 P. E. Kreter, jun., D. W. Meek, and G. G. Christoph, *J. Organomet. Chem.*, 1980, **188**, C27; G. N. Mott, N. J. Taylor, and A. J. Carty, *Organometallics*, 1983, **2**, 447.
4 V. D. Bianco and S. Dorronzo, *Inorg. Synth.*, 1976, **16**, 161.
5 W. Kuchen and H. Buckwald, *Chem. Ber.*, 1951, **91**, 2296.
6 B. F. G. Johnson, J. Lewis, J. N. Nicholls, J. Puga, P. R. Raithby, M. J. Rosales, M. McPartlin, and W. Clegg, *J. Chem. Soc., Dalton Trans.*, 1983, 277.
7 G. M. Sheldrick, 'SHELX, Program for Crystal Structure Determination,' University of Cambridge, 1976.
8 'International Tables for *X*-Ray Crystallography,' Kynoch Press, Birmingham, 1974, vol. 4.
9 W. D. S. Motherwell and W. Clegg, 'PLUTO, Program for Plotting Molecular and Crystal Structures,' Universities of Cambridge and Gottingen, 1978.
10 A. G. Cowie, B. F. G. Johnson, J. Lewis, J. N. Nicholls, P. R. Raithby, and M. J. Rosales, *J. Chem. Soc., Dalton Trans.*, 1983, 2311.
11 J. Evans, B. P. Gracey, L. R. Gray, and M. Webster, *J. Organomet. Chem.*, 1982, **240**, C61.
12 M. I. Bruce, B. W. Skelton, A. H. White, and M. L. Williams, *J. Chem. Soc., Chem. Commun.*, 1985, 744.
13 J. W. Kolis, F. Basolo, and D. F. Schriver, *J. Am. Chem. Soc.*, 1982, **104**, 5626.
14 J. Evans, *J. Chem. Soc., Dalton Trans.*, 1978, 25.
15 B. P. Gracey, Ph.D. Thesis, University of Southampton, 1983.
16 S. L. Cook and J. Evans, *J. Chem. Soc., Chem. Commun.*, 1983, 713.

Received 2nd September 1985; *Paper* 5/1502